Proceedings of the 7th International Conference on Fluid Flow, Heat and Mass Transfer (FFHMT'20)
~~Niagara Falls, Canada~~ Virtual Conference – November, 2020
Paper No. 194
DOI: 10.11159/ffhmt20.194

Design Algorithm Evaluation of Swirler-Injector Systems in Liquid-Burning Combustion Chambers

Arash Mousemi[1], Sepehr Mosadegh[2], Alireza Khademi[2], Giancarlo Sorrentino[3]
[1]Department of Mechanical Engineering, University of British Columbia
Vancouver, Canada
arash.mousemi@alumni.ubc.ca
[2]Department of Aerospace Engineering, Sharif University of Technology
Azadi Ave, Tehran, Iran
sepehr.mosadegh@ae.sharif.edu; khademi_alireza@ae.sharif.edu
3Department of Chemical, Materials and Industrial Production Engineering, University of Naples
P.le Tecchio 80, 80125 Naples, Italy
g.sorrentino@unina.it

Abstract **-** Liquid-burning combustion chambers have a wide range of applications in propulsion systems and energy conversion processes. The growing need for reliable and low-NOx combustion systems highlights the role of high-performance burners, where the main design criticalities are related to injectors and swirlers. In the current study, an algorithm for coupling the design procedure of pressure-swirl injectors and axial swirlers is introduced. Also, this algorithm emphasizes the interrelation between the design parameters of these two components via employing the length of the recirculation zone as the coupling parameter for building a relationship between the design characteristics of the injector and swirler. We have employed Maximum Entropy Formalism (MEF) to obtain a prediction for the distribution of diameters and velocities of fuel droplets, which takes part as a criterion in the design procedure of the injector.

Keywords**:** Swirler-injector systems; combustion chambers; energy conversion; pressure-swirl injector; axial swirler.

Nomenclature

A_0	=	cross section area of discharge nozzle of injector (m^2)
A_{ft}	=	area of flame tube (m^2)
A_p	=	cross section area of tangential entry passages of injector (m^2)
A_{ref}	=	reference area in combustion chamber (m^2)
A_{sw}	=	front area of swirler (m^2)
C_d	=	injector discharge coefficient (dimensionless)
c	=	chord of swirler vanes (m)
D_0	=	initial diameter of a fuel droplet (m)
D_{hub}	=	hub diameter of swirler (m)
D_L	=	ligament diameter (m)
D_{tip}	=	tip diameter of swirler (m)
d_m	=	mass mean diameter of the spray (m)
L_e	=	required length for evaporation of one droplet in primary zone (m)
L_{RZ}	=	length of the recirculation zone (m)
L_r	=	required length for the travel of one droplet from injector tip to combustor walls (m)
$\dot{m}$	=	mass flowrate (kg/s)
$\dot{m}_3$	=	mass flowrate of air entering combustion chamber (kg/s)
$\dot{m}_{sw}$	=	mass flowrate of air entering swirlers (kg/s)
N_{bu}	=	number of burner systems in the combustor (dimensionless)
Oh	=	Ohnesorge number (dimensionless)

P = static pressure (Pa)
p_i = the probability of occurrence of the state i (dimensionless)
q_{ref} = reference dynamic head of the flow entering combustion chamber (Pa)
S = Shannon entropy (dimensionless)
S_e = energy source-term (kg.m^2/s^3)
$\bar{s}_e$ = dimensionless energy source-term (dimensionless)
S_m = mass source-term (kg/s)
$\bar{s}_m$ = dimensionless mass source-term (dimensionless)
S_{mv} = momentum source-term (kg.m/s^2)
$\bar{s}_{mv}$ = dimensionless momentum source-term (dimensionless)
SMD = Sauter mean diameter (m)
SMD_d = desired Sauter mean diameter for injector (m)
t = liquid film thickness at the nozzle tip of injector (m)
t_e = required time for evaporation of one droplet in primary zone (s)
t_r = required time for the travel of one droplet from injector tip to combustor walls (s)
V_0 = velocity of liquid sheet at the nozzle tip of injector (m/s)
WT = wall thickness of the atomizer (m)
δ_{ij} = Kronecker Delta Function (dimensionless)
μ = dynamic viscosity (Pa.s)
ρ_a = density of air (kg/m^3)
ρ_f = density of fuel (kg/m^3)
σ = surface tension of fuel (N/m)

Subscripts
f = fuel

1. Introduction

The fulfilment of several needs in the aviation and energy conversion industries is currently faced with several constraints that are continuously changing the possible scenarios of the near future energy market.

The increasing share of renewable energy with a drastic reduction of greenhouse gas emissions requires the development of reliable burner systems that simultaneously realize the flexibility, high efficiency and very low pollutant emissions [1]. In this context, the assembly and proper design of injector and swirler are essential steps in new burner conceptions as they affect the stabilization and performance of the flame in the expected zone. Pressure-swirl injectors are frequently utilized in various combustion systems and are one of the most common types of atomizers due to their simplicity [2]. Liquid fuel is fed to the atomizer via tangential entry ports which induces a centrifugal force to the fluid flow and results in the generation of a gas-core vortex in the atomizer [3]. Therefore, fuel exits from the injector in the form of a hollow cone and then breaks into smaller ligaments and finally droplets.

There are several theoretical and experimental models available on this kind of atomization technique [4]. Lacava et al. [5] proposed an algorithm for the design of pressure-swirl atomizers and validated this algorithm with experimental data. Bazarov and Yang [6] studied the dynamics of the pressure-swirl atomizers of the liquid-propellant rocket engines. Sumer et al. [7] investigated the structure of the flow inside a pressure-swirl atomizer with both experimental techniques and computational fluid dynamics (CFD) tools. The research of Couto et al. [8] revealed a theoretical formulation for predicting the Sauter Mean Diameter of the droplets produced by the pressure-swirl injectors.

Axial swirlers are prevalently utilized in the aero-engines to stabilize the flame by inducing an adverse pressure gradient that results in the creation of a recirculation zone in the primary section of the combustion chamber [9]. The strength of the induced swirl is required to be higher than a minimum value to ensure the flame stability. Meanwhile, the air that is fed to the combustor through the swirler collaborates with the cooling of the liner walls. Therefore, the detailed design of the swirlers plays a crucial role in the performance of combustion chamber. Some studies have been performed on determining the working principles of swirlers [10, 11].

The major limitation of the studies reviewed in this work is the lack of reciprocal interrelation between the design methodology of injector and swirler. Indeed, the performance of these two components is highly dependent on each other. In this study, we introduce an algorithm for the design of the burner as an integrated system. This technique consists of a design method for pressure-swirl injectors and a prediction for the distribution of velocities and diameters of the fuel droplets generated by the atomizer via Maximum Entropy Formalism (MEF). Also, a procedure for the design of axial swirlers is obtained based on the characteristics of the injector. Then, in this algorithm, the injector is redesigned according to the performance parameters of the achieved swirler, and this cycle is repeated up to an optimal point where the geometrical parameters of the designed burner system converge.

2. Technical Data of the Combustion Chamber

The operative conditions and geometrical parameters of the combustion chamber have essential roles in determining the designing criteria of the injector and swirler. Indeed, the burner system must be conceived after the preliminary design of the combustor which specifies the information about its sizing, air partitioning, total pressure loss in the combustion chamber and temperature of primary zone as input data required for the algorithm proposed in this paper. The algorithm is applied in order to design the burner system used in an annular Kerosene-burning combustion chamber with the technical characteristics summarized in Table 1.

Table 1: Characteristics of the combustor that are related to the burner design.

Parameter	Quantity	Parameter	Quantity	Parameter	Quantity
Combustor Reference Area	0.3135 m^2	Liner Diameter	15.13 cm	Liner outer wall diameter	61.3 cm
Air mass flow rate for all swirlers	1.356 kg/s	Fuel mass flow rate for all injectors	0.3168 kg/s	Pressure Loss Factor	20
Total pressure of the flow exiting from compressor	7 bar	Static pressure of the flow exiting from compressor	6.785 bar	Temperature in primary zone	1800 K

Before describing the method of designing the injector and swirler, it is crucial to decide on the number of burners employed in the combustor, which can be determined by:

$$N_{bu} = \mathrm{ceil}\left(\frac{2\pi}{2\sin^{-1}\left(\frac{D_{ft}}{D_{ft,2} - D_{ft}}\right)}\right) \tag{1}$$

Where D_{ft} and $D_{ft,2}$ are represented in Figure 1.

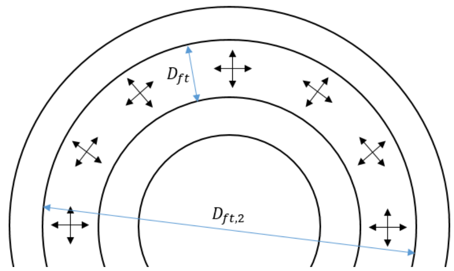

Fig. 1: The cross-sectional schematic of the combustor which illustrates the reference diameters.

3. Design of Pressure-Swirl Injector

To design a pressure-swirl injector, the geometrical parameters represented in Figure 2 are needed to be determined. In the current study, the duty of the injector is assumed to be the production of desired distribution for diameters as well as axial and radial velocities of the droplets to ensure that all of them would be evaporated in the recirculation zone and take part in combustion. The spray cone semi-angle (θ) suggests an interrelation between the axial and radial components of the droplet velocities, and in section 6, a relation between this parameter and the diameter of the swirler is introduced. However, at the first step, the swirler diameter is unknown, hence, we chose 45^{o} as the initial value of the spray cone semi-angle to start the design procedure. The magnitude of this angle is crucial for the residence time of the droplets in the primary zone, and is linked to the desired distribution of droplet sizes.

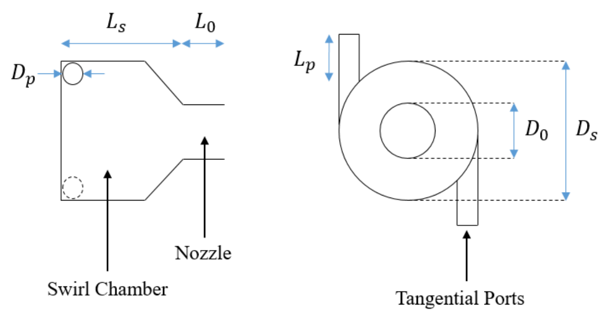

Fig. 2: Geometrical parameters for the design of injector.

In the next stage, the proper value for L_s/D_s which commits to two competing effects should be chosen. It is essential to opt for a value that is high enough to stabilize the flow. This stabilization results in the generation of a uniform vortex sheet, nonetheless, the pressure loss in the atomizer will be increased by increasing this ratio [5]. Elkotb et al. [12] suggested that 1 is an appropriate value for this parameter, and in the design procedure, this recommended value for L_s/D_s is selected. Furthermore, a proper value is required to be assigned to L_0/D_0 as another dimensionless geometrical parameter.

The effective flow area in the injector is characterized by the Flow Number which is a key parameter for calculating the value of geometrical unknowns, and it is defined in Equation (2) [2]:

$$\mathrm{FN} = \frac{\dot{m}_f}{\sqrt{\rho_f \Delta P}} \tag{2}$$

In order to proceed, D_0 should be specified, so, an initial guess is needed to be made for this parameter, and modified until the desired SMD is achieved. A value is assigned to D_0 in each iteration, and by evaluating this variable, discharge coefficient which stands for the pressure losses aroused in the nozzle flow passages and the effective cross-sectional area occupied by the fuel flow can be calculated. This variable is defined as [13]:

$$C_d = \frac{\dot{m}_f}{A_0\sqrt{2\rho_f \Delta P}} \tag{3}$$

Next, X parameter is defined as the ratio between the area of the core air and total area of the discharge orifice. Assuming Assuming that all of the pressure difference made by the fuel pump turns into dynamic pressure of the fuel jet at the nozzle nozzle tip, and using definition brought in Equation (2), X can be related to other atomizer's characteristics through Equation Equation (4) [5]:

$$X = 1 - \frac{FN}{\pi\sqrt{2}\left(\frac{D_0}{2}\right)^2} \tag{4}$$

Using the value obtained for C_d, X and θ, the value of $A_p/(D_s D_0)$ is governed by [13]:

$$\frac{A_p}{D_s D_0} = \frac{\frac{\pi}{2} C_d}{(1+\sqrt{X})\sin(\theta)} \tag{5}$$

For the next step, the liquid film thickness at the nozzle tip of the atomizer is estimated by Equation (6) which is an empirical correlation suggested by Couto et al. [8]:

$$t = \frac{0.00805.FN.\sqrt{\rho_f}}{D_0 \cos\theta} \tag{6}$$

Again, neglecting pressure losses in the injector and knowing the quantity of ΔP, the velocity of liquid sheet at the nozzle tip is given by Equation (7):

$$V_0 = \sqrt{\frac{2\Delta P}{\rho_f}} \tag{7}$$

The correlation offered by Couto et al. [8] is employed to find the diameter of the ligaments generated in the primary step of atomization and then Equation (8) is used for calculating SMD of the droplets formed by the injector.

$$SMD = 1.89 D_L (1 + 3Oh)^{\frac{1}{6}} \tag{8}$$

SMD of the droplets should be equal to or smaller than the desired value, besides, $A_p/D_s D_0$ is preferred to be between 0.19 and 1.21. Hence, we can make use of the value of these parameters as two primary checkpoints for the injector design.

4. Maximum Entropy Formalism

In MEF, the information theory is used to characterize the velocity and size distribution of the droplets generated by the injector. The theory proposes that there is a condition in which the entropy of the system reaches its maximum, and results in the distribution with the most possibility under the restriction of constraints applied due to the nature of the phenomena [14]. Shannon [15] proposed the relationship represented in Equation (9) to set a link between the information entropy and probability distribution.

$$S = -\sum_i p_i \ln(p_i) \tag{9}$$

To show that the probability is a function of droplet size and velocity, p_i should be replaced by p_{ij} which indicates the probability of having a droplet with diameter of D_i and velocity of V_j. Throughout the present work, all the fuel droplets are assumed to be spherical, and their diameters and velocities are normalized by the mass mean diameter (d_m) of the droplets and the liquid film velocity in the jet direction at the nozzle exit, respectively.

$$\bar{D}_i = \frac{D_i}{d_m} \tag{10}$$

$$\bar{V}_j = \frac{V_j}{V_0/\cos\theta} \tag{11}$$

There are some constraints forced by the necessity of number balance, mass balance, momentum balance and energy balance of the droplets. The number balance of the droplets suggests that the summation of the probabilities should be to 1 as represented in Equation (12):

$$\sum_j \sum_i p_{ij} - 1 = 0 \tag{12}$$

Moreover, the mass, momentum, and energy balance for the droplets impose three following equations [16]:

$$\sum_j \sum_i p_{ij}\, \bar{D}_i^{\,3} - (1 + \bar{s}_m) = 0 \tag{13}$$

$$\sum_j \sum_i p_{ij}\, \bar{D}_i^{\,3} \bar{V}_j - (1 + \bar{s}_{mv}) = 0 \tag{14}$$

$$\sum_j \sum_i p_{ij}\, \bar{D}_i^{\,3} \bar{V}_j^{\,2} - (1 + \bar{s}_e) = 0 \tag{15}$$

Here $\bar{s}_m = S_m/\dot{m}_f$ is the dimensionless source-term for mass exchange between the liquid jet and the surrounding gas, and takes care of the fuel evaporation rate at the primary and secondary phases of the liquid film breakup process. In order to simplify the model used for this term and to reach higher reliability for the design algorithm, more critical condition in which droplets have shorter time to be vaporized, and droplet evaporation starts after completion of breakup process is assumed. This assumption implies that the dimensionless mass source-term should be neglected through the rest of this work. $\bar{s}_{mv} = (S_{mv}\cos\theta)/(\dot{m}_f V_0)$ denotes the dimensionless momentum loss of the liquid particles due to the drag force imposed by the surrounding gas inside the combustion chamber. In addition, $\bar{s}_e = (S_e \cos^2\theta)\,/(\dot{m}_f V_0^2)$ is the dimensionless energy source-term for balancing the equation of energy conservation, and accounts for the rate at which the liquid particles lose their kinetic energy. To set a value for $\bar{s}_{mv}$ the trial-and-error method applied by Mondal et al. [14] is used to achieve a reasonable distribution. Moreover, they suggested Equation (16) which accounts only for transformation of the kinetic energy to the interfacial free energy of fuel droplets in order to obtain the value of $\bar{s}_e$.

$$\bar{s}_e = \frac{12\sigma\cos^2\theta}{\rho_f V_0^2}\left(\frac{1}{3t\cos\theta} - \frac{1}{SMD}\right) \tag{16}$$

All of the parameters that appeared on the right-hand side of this equation are determined during the atomizer design procedure.

To maximize the entropy of the system, Kim et al. [17] made use of the Lagrange multipliers method and demonstrated that the PDF should be in the form of,

$$f = f_0 \times \exp\left(-(\lambda_1 + \lambda_2\bar{D}^3 + \lambda_3\bar{D}^3\bar{V} + \lambda_4\bar{D}^3\bar{V}^2)\right) \tag{17}$$

Where f_0 is the PDF of prior droplet sizes; λ_1, λ_2, λ_3 and λ_4 are the Lagrange multipliers which are essential to be calculated for specifying the joint PDF.

As it was mentioned, the droplet diameters are normalized by d_m, and to characterize the distribution of the diameters of the droplets, mass mean diameter is required, which is calculated by [18]:

$$d_m = SMD \times \int_0^{\bar{V}_{max}} \int_0^{\bar{D}_{max}} f\bar{D}^2\, d\bar{D}\, d\bar{V} \tag{18}$$

Therefore, the size and velocity distribution for the droplets which is necessary for designing the burner system as an integrated system is obtained.

5. Design of Flat-Vane Axial Swirler

To accomplish the preliminary design of a flat-vane axial swirler, the geometrical parameters shown in Figure 3 are required to be specified. The functionality of the swirler is dependent on the formation of a low-pressure recirculation zone which occurs in highly-swirled flows. Hence, the crucial criteria for designing a swirler is to induce a sufficient swirl to the air passing through it to cause a vortex breakdown in the combustor. Firstly, an initial value should be fixed for the angle of the swirler vanes with respect to the axial direction (β_{sw}) which is considered to be between $30^o$and 60^o. Moreover, pressure loss factor of the airflow due to the passage through the swirler is needed to be determined. It is suggested to consider the total pressure loss in the swirler equal to 3% to 4% of the total pressure of the air entering the combustion chamber [19]. By allocating a value to these parameters, the total area of the swirlers can be calculated by:

$$A_{sw} = \sqrt{\frac{A_{ref}^2}{\left[\frac{\Delta P_{sw}}{q_{ref}K_{sw}}\left(\frac{\dot{m}_3}{\dot{m}_{sw}}\right)^2 + \left(\frac{A_{ref}}{A_{ft}}\right)^2\right]\cos^2\beta_{sw}}} \tag{19}$$

Where the appropriate value for K_{sw} is 1.3 for a flat-vane swirler and 1.15 for a curved-vane one [19]. On the other hand, the area of the swirler is related to the geometrical characteristics of it through Equation (20):

$$A_{sw} = N_{bu}\left[\frac{\pi}{4}\left(D_{tip}^2 - D_{hub}^2\right) - 0.5n\delta\left(D_{tip} - D_{hub}\right)\right] \tag{20}$$

Here n and δ represent the number of blades used in each swirler and blade thickness, respectively. These parameters are needed to be selected according to the technology of manufacturing. The number of blades is chosen between 8 to 16, and the blade thickness is set between 0.7 mm to 1.5 mm. In addition, having the geometrical characteristics of the injector, we can obtain the value of hub diameter of the swirler by,

$$D_{hub} = D_s + 2WT \tag{21}$$

In which WT is the wall thickness of the atomizer. After determining the appropriate values of β_{sw}, D_{hub}, D_t, n and δ, the chord length of the swirler vanes is the only geometrical parameter of this component left unknown, and can be determined using no see-through rule which suggests that the gap between swirler vanes should not be observable by looking at the burner in direction parallel to its axis. Therefore, the chord length can be calculated by:

$$c = \frac{\pi D_{tip}}{n}\csc(\beta_{sw}) \tag{22}$$

Moreover, the recirculation zone angle (θ_{RZ}) which is illustrated in Figure 3 is related to the features of the swirler with:

$$\theta_{RZ} = \cos^{-1}\left[\frac{-D_{ft}\left(D_{ft} - 2D_{tip}\right) - \left(D_{ft} - 4L_{RZ}\right)\sqrt{D_{ft}^2 - 4D_{ft}D_{tip} + 4D_{tip}^2 - 8D_{ft}L_{RZ} + 16L_{RZ}^2}}{2D_{ft}^2 - 4D_{ft}D_{tip} + 4D_{tip}^2 - 8D_{ft}L_{RZ} + 16L_{RZ}^2}\right] \tag{23}$$

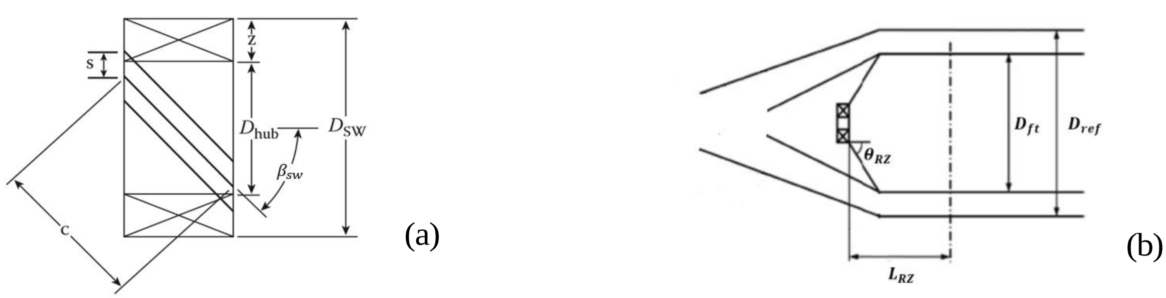

Fig. 3: (a) Geometrical parameters for the design of swirler, (b) Recirculation zone wall angle.

In practice, the characteristics of injector and swirler are interrelated, and they have a considerable impact on the performance of each other. Therefore, obtaining a relationship between the features of these two components in the design procedure of the burner system is essential, and is discussed in the next section.

6. The Burner System Design Procedure

Our aim in this section is to couple the design procedure of injector and swirler and propose a method for designing the whole burner simultaneously. The upper limit for SMD should be revised according to the time which droplets have before reaching the liner walls. To obtain the value of these two parameters, we should first specify the path droplets travel through, and introduce a model for evaporation of them in the combustor. After the rudimentary design of the the spray cone semi-angle should be revised as,

$$\theta = \tan^{-1}(\frac{D_{ft}}{4D_{sw}}) \tag{24}$$

Therefore, the required time for the droplets to travel from the injector nozzle to the combustor walls is calculated via Equation (25):

$$t_r = \frac{2D_{sw}}{V_0} \tag{25}$$

On the other hand, Chin and Lefebvre [20] suggested using Equation (26) for determining the required time for evaporation of a droplet with the initial diameter of D_0.

$$t_e = \frac{D_0^2}{\lambda_{eff}} \tag{26}$$

Here λ_{eff} denotes the effective evaporation constant for the fuel droplets which takes care of both heat-up and steady-state periods of drop evaporation discussed in [2]. This parameter is a function of the pressure and temperature of the combustor, and velocity of the droplet relative to surrounding air and boiling point of the fuel. The initial temperature of the fuel flow influences the heat-up phase which is of minor importance compared to the steady-state period of evaporation.

To do so, the droplet diameter which is higher than the size of 90% of the droplets (D_{90}) and the velocity of the droplet which is higher than the velocity of 90% of them (V_{90}), are calculated through the joint PDF specified by MEF. The length that a droplet with the diameter of D_{90} and velocity of V_{90} required to evaporate in the combustor is calculated by:

$$L_e = \frac{D_{90}^2}{\lambda_{eff}} \times V_{90} \tag{27}$$

This length has to be smaller than the length that droplets travel to reach the liner walls, which can be described as:

$$L_r = \frac{D_{ft}}{2\sin\theta} \tag{28}$$

If $L_e > L_r$, we should reduce SMD_d and repeat all of the procedures introduced in sections 3, 4 and 5 for the design of injector and swirler and continue the cycle till L_e becomes smaller than L_r.

7. Results

To evaluate the developed methodology established in this paper, we applied this procedure to design a burner system. The results of the geometrical parameters of the injector and swirler are summarized in Table 2. In addition, the PDF for the diameters and velocities of the droplets is illustrated in Figure 4. Each of the empirical correlations used in this work include some level of uncertainty, and the employed analytical expressions have added some unphysical assumptions to our design procedure. Thus, departure from the physics is expected for the reported results. An error propagation analysis can be conducted in the future works to have a prediction for the uncertainties present in the design parameters. The shape of PDF represents that the majority of the fuel droplets have velocities and diameters which are near to the mean values, and the probability of finding a droplet with a diameter 3 times bigger than the mean value is negligible.

Table 2: Design parameters for the burner.

N_{bu}	10	SMD	37.12 μm	$A_p/(D_s D_0)$	0.1978
θ	32.34°	D_0	3.5 mm	D_s/D_0	7.99
ΔP	4 bar	D_s	2.8 cm	t	0.136 mm

n_p	2	β	52^o	D_{hub}	3.1 cm
D_p	3.5 mm	n	12	SN	1.017
δ	0.7 mm	D_{tip}	5.97 cm	θ_{RZ}	33.01^o
D_{hub}/D_{tip}	0.546	D_{tip}/D_{ft}	0.395	c	1.98 cm

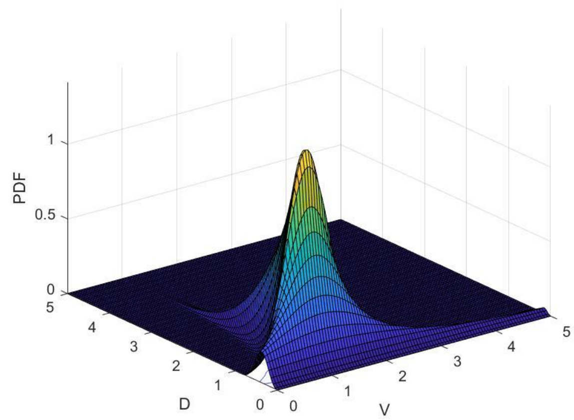

Fig. 4: Probability density function for the distribution of diameter and velocity of droplets.

8. Conclusion

In the context of low-NOx combustion systems, the present study introduced an optimization procedure coupled with a design algorithm for pressure-swirl injectors and a prediction for the distribution of velocities and diameters of fuel droplets generated by the atomizer via Maximum Entropy Formalism (MEF). Moreover, a procedure for the design of axial swirlers was obtained based on the characteristics of the injector. Then, in this algorithm, injector was redesigned according to the performance parameters of the achieved swirler, and this cycle was repeated up to an optimal point where the geometrical parameters of the designed burner system converge. The injector and swirler conceptions were coupled to the whole burner design simultaneously. Moreover, the distribution of the diameters and velocities of the droplets which were obtained through the MEF were considered in the design procedure. All of the equations were extracted from publications with numerical or experimental verification. Future improvements of the model will require validation data to prove the functionality of the designed system.

References

[1] B. Diczfalusy *et al.*, "Energy Technology Perspectives 2012: Pathways to a Clean Energy System (ETP 2012)," ed: International Energy Agency: Paris, 2012.

[2] A. H. Lefebvre and D. R. Ballal, *Gas turbine combustion: alternative fuels and emissions*. CRC press, 2010.

[3] X. Chen and V. Yang, "Effect of ambient pressure on liquid swirl injector flow dynamics," *Physics of Fluids,* vol. 26, no. 10, p. 102104, 2014.

[4] W. Ipp *et al.*, "Spray formation of high pressure swirl gasoline injectors investigated by two-dimensional Mie and LIEF techniques," *SAE transactions*, pp. 503-515, 1999.

[5] P. T. Lacava, D. Bastos-Netto, and A. P. Pimenta, "Design procedure and experimental evaluation of pressure-swirl atomizers," in *24th international congress of the aeronautical sciences*, 2004.

[6] V. G. Bazarov and V. Yang, "Liquid-propellant rocket engine injector dynamics," *Journal of Propulsion and Power,* vol. 14, no. 5, pp. 797-806, 1998.

[7] B. Sumer, N. Erkan, O. Uzol, and I. Tuncer, "Experimental and numerical investigation of a pressure swirl atomizer," in *Proceedings of 12th ICLASS Conference,* 2012: Ilass Europe Heidelberg, Germany.

[8] H. Couto, J. Carvalho Jr, and D. Bastos-Netto, "Theoretical formulation for sauter mean diameter of pressure-swirl atomizers," *Journal of Propulsion and power*, vol. 13, no. 5, pp. 691-696, 1997.

[9] Y. Fu, S.-M. Jeng, and R. Tacina, "Characteristics of the swirling flow generated by an axial swirler," in *ASME Turbo Expo 2005: Power for Land, Sea, and Air*, 2005: American Society of Mechanical Engineers Digital Collection, pp. 517-526.

[10] G. B. Hegde, B. Khandelwal, V. Sethi, and R. Singh, "Design, evaluation and performance analysis of staged low emission combustors," in *ASME Turbo Expo 2012: Turbine Technical Conference and Exposition*, 2012: American Society of Mechanical Engineers Digital Collection, pp. 867-875.

[11] Y. Fu, S.-M. Jeng, and R. Tacina, "Confinement effects on the swirling flow generated by a helical axial swirler," in *44th AIAA Aerospace Sciences Meeting and Exhibit*, 2006, p. 545.

[12] M. Elkotb, N. Rafat, and M. Hanna, "The influence of swirl atomizer geometry on the atomization performance," in *Proceedings of the 1st International Conference on Liquid Atomization and Spray Systems*, 1978, pp. 109-115.

[13] J. J. Chinn, "An appraisal of swirl atomizer inviscid flow analysis, Part 1: The principle of maximum flow for a swirl atomizer and its use in the exposition and comparison of early flow analyses," *Atomization and Sprays*, vol. 19, no. 3, 2009.

[14] D. Mondal, A. Datta, and A. Sarkar, "Droplet size and velocity distributions in a spray from a pressure swirl atomizer: application of maximum entropy formalism," *Proceedings of the Institution of Mechanical Engineers, Part C: Journal of Mechanical Engineering Science*, vol. 218, no. 7, pp. 737-749, 2004.

[15] C. E. Shannon, "A mathematical theory of communication," *Bell system technical journal*, vol. 27, no. 3, pp. 379-423, 1948.

[16] R. Tate and W. Marshall, "Atomization by centrifugal pressure nozzles," *Chemical Engineering Progress*, vol. 49, no. 4, pp. 169-174, 1953.

[17] W. T. Kim, S. K. Mitra, X. Li, L. Prociw, and T. Hu, "A predictive model for the initial droplet size and velocity distributions in sprays and comparison with experiments," *Particle & Particle Systems Characterization: Measurement and Description of Particle Properties and Behavior in Powders and Other Disperse Systems*, vol. 20, no. 2, pp. 135-149, 2003.

[18] S. Nukiyama, "Experiments on the atomization of liquids in an air stream, report 3, on the droplet-size distribution in a atomized jet," *Trans. Soc. Mech. Eng. Japan*, vol. 5, pp. 62-67, 1939.

[19] D. Spalding, "Combustion Aerodynamics. By JM B EéER and NA C HIGIER. Applied Science Publishers Ltd, 1972. 264 pp.£ 7.00," *Journal of Fluid Mechanics*, vol. 54, no. 4, pp. 762-762, 1972.

[20] J. Chin and A. Lefebvre, "Effective values of evaporation constant for hydrocarbon fuel drops," in *Proceedings of the 20th Automotive Technology Development Contractor Coordination Meeting*, 1982, pp. 325-331.